Numerical simulations for astrophysical plasma jets

Ioana Duțan

Institute of Space Science, Bucharest-Măgurele, Romania

work with:
K.-I. Nishikawa, A. Meli, C. Köhn, N. MacDonald,
Y. Mizuno, O. Kobzar, J. Gómez, K. Hirotani

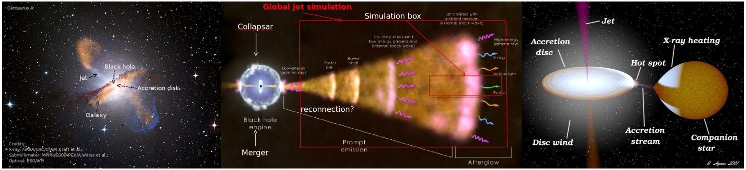

Credits:
X-ray: NASA/CXC/CfA/R.Kraft et al.;
Submillimeter: MPIfR/ESO/APEX/A.Weiss et al.;
Optical: ESO/WFI

Outline

Outline

Outline

Outline

How do we see deep into the Universe?

Optic: NASA/ESA: Hubble Telescope (1990-])

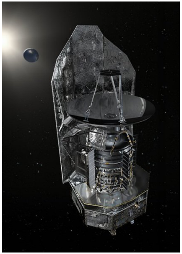

Infrared: ESA: Herschel Telescope (2009-2013)

Radio: NRAO: VLA (1980-)

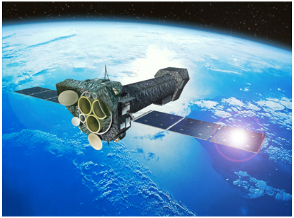

X-ray: ESA: XMM-Newton (1999-)

Event Horizon Telescope (EHT)

- 8 telescopes around the world joined together to create a virtual Earth-sized telescope
- observes (mm)-synchrotron radiation at a frequency of 230 GHz (a wavelength of 1.3 mm) using the technique of Very Long Baseline Interferometry (VLBI)

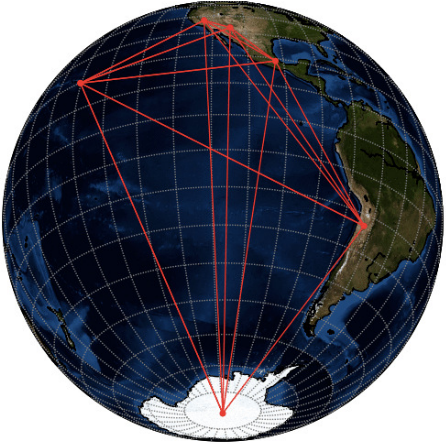

What we do see comes from emission of radiation

- Electromagnetic spectrum

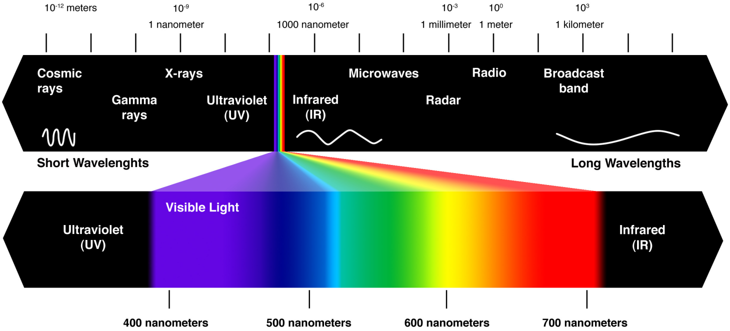

What we do see comes from emission of radiation via different mechanisms

- Line emission over a very narrow frequency range - usually due to the discrete (quantised) transitions in the energy states of atoms or molecules
  - hydrogen 21-cm line (galaxies)
  - H is the most abundant element in the Universe: $\sim 75\%$; He: $\sim 25\%$
  - recombination lines, MASERs (e.g., dense molecular clouds, around late-type stars)
- Continuum emission over a very broad frequency range
  - thermal radiation
    - black-body radiation
    - Bremsstrahlung radiation
  - non-thermal radiation
    - synchrotron radiation
    - (inverse)-Compton scattering

Basic equations for observing radiation

- a telescope detector (of infinitesimal area $d\sigma$) observing a source measures an energy dE from within the solid angle $d\Omega$ flows through the projected area $\cos\theta d\sigma$ in time dt and in a narrow frequency band of width $d\nu$

  $$dE = I_\nu \cos\theta d\sigma d\Omega dt d\nu, \qquad (1)$$

  where I_ν is the specific intensity (in units of W m^{-2} Hz^{-1} sr^{-1}), a property which is fundamental to the source

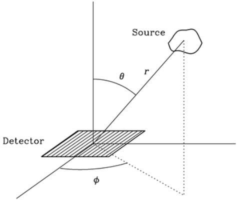

- power is defined as the flow of energy per unit time: $P = \frac{dE}{dt}$

Basic equations for observing radiation

- if a source is discrete (subtends a well-defined solid angle), the spectral power received by a detector of unit projected area is called the flux density S_ν (in units of W m^{-2} Hz^{-1}) of the source:

$$S_\nu = \frac{dP}{d\sigma d\nu} = I_\nu \cos\theta d\Omega \tag{2}$$

- integrating over the solid angle subtended by the source yields

$$S_\nu \equiv \int_{\text{source}} I_\nu(\theta,\phi)\cos\theta d\Omega \tag{3}$$

- if the source angular size is $\ll 1$ rad, $\cos\theta \approx 1$, the expression for flux density is much simpler:

$$S_\nu \approx \int_{\text{source}} I_\nu(\theta,\phi) d\Omega \tag{4}$$

Blackbody radiation

- all objects with a temperature above absolute zero (0 K) emit energy in the form of electromagnetic radiation
- a blackbody is a theoretical or model body which absorbs all radiation falling on it, reflecting or transmitting none. Real ones transmit some radiation
- this results from the tiny random motions of particles, atoms and molecules, in the object, which can be described by a thermal energy

- spectral distribution of the thermal energy radiated by a blackbody depends only on its temperature

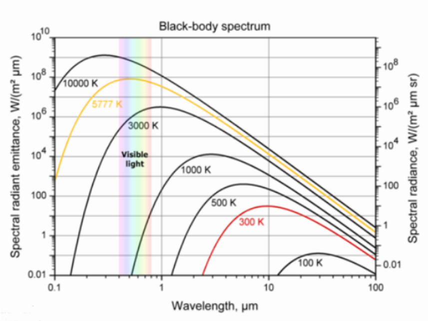

Blackbody radiation

- all objects with a temperature above absolute zero (0 K) emit energy in the form of electromagnetic radiation
- this results from the tiny random motions of particles, atoms and molecules, in the object, which can be described by a thermal energy

- radio to far-IR spectrum of starburst galaxy M82
- thermal dust emission dominates at hight freqs

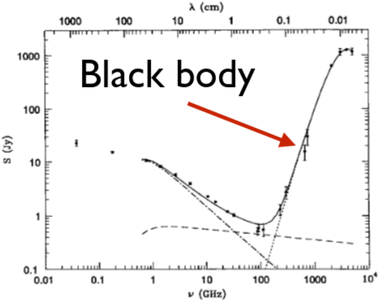

Bremsstrahlung (free-free) radiation

An un-magnetised diffuse, ionised source (HII regions) produces bremsstrahlung (free-free) emission.

It is produced by the deflection (acceleration) of a charged particle (usually an electron in astrophysical situations) in the electric field of another charged particle (usually an atomic nucleus).

Bremsstrahlung (free-free) radiation

- contribution from free-free emission is indicated by the nearly-flat dashed line
- free-free abs HII regions distributed throughout the galaxy absorb some of the synchrotron radiation and flattens the overall spectrum

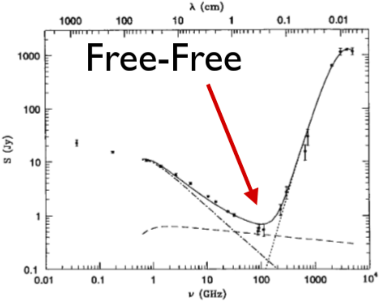

Synchrotron radiation

- a relativistic charged particle which is accelerated in a region having a magnetic field emits synchrotron radiation
- particle gyrates along the magnetic field lines
- electrons are better emitters that protons as the latter are heavier

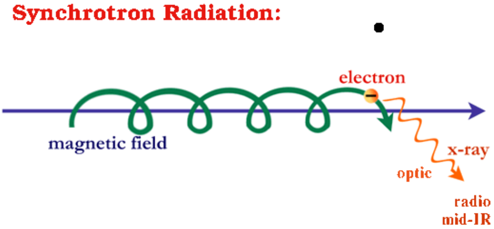

Synchrotron radiation

- Acceleration mechanisms produce electrons with **power-law distribution** in energies.
- Assuming photons emit only at ν_c

$$n(\gamma)\mathrm{d}\gamma = n_0\gamma^{-p}\mathrm{d}\gamma$$

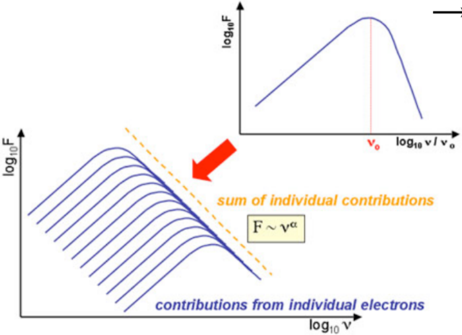

→ Power-law distribution in energies generates power-law spectrum

Critical frequency:

$$\nu_c = \frac{3\gamma^2 eB}{4\pi m_e}$$

Synchrotron decay time:

$$\tau = \frac{E}{P} \propto \frac{\gamma m c^2}{B^2\gamma^2} \propto \frac{1}{B^2\gamma}$$

Continuous spectrum of light & emission and absorption lines

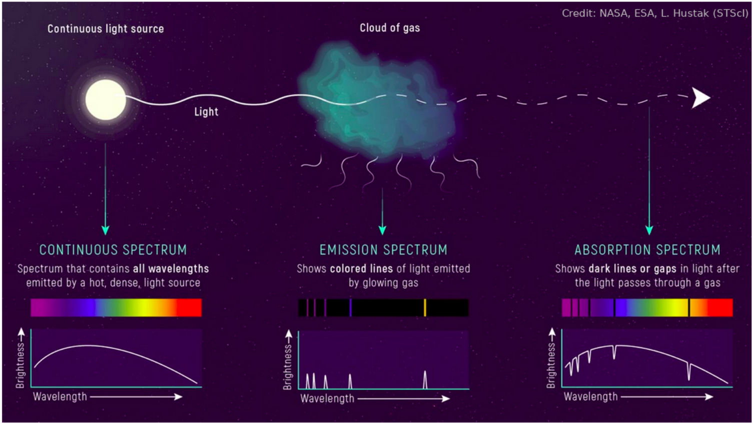

Credit: NASA, ESA, L. Hustak (STScI)

Line emission

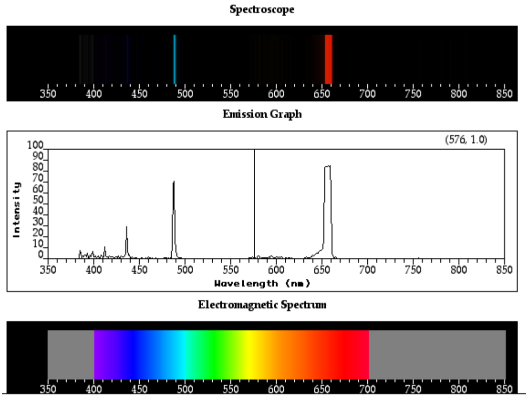

- Hydrogen emission spectrum: consists of 4 emission lines ("its signature")

Spectral lines (Bohr's model for hydrogen atom)

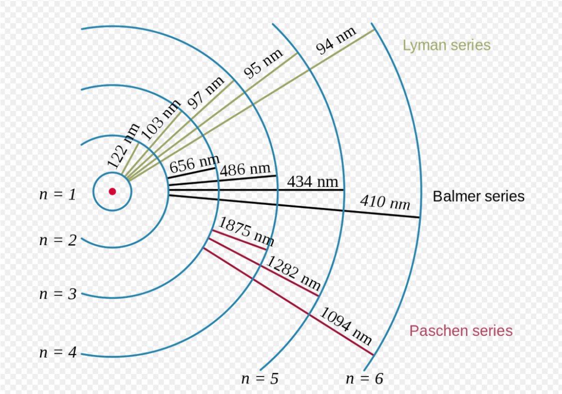

wiki

Line absorption

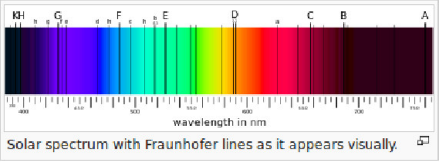

Solar spectrum with Fraunhofer lines as it appears visually.

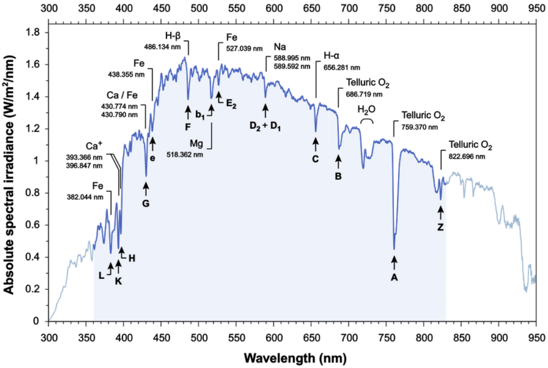

- Sun atmosphere absorption spectrum

Atomic hydrogen 21-cm line emission

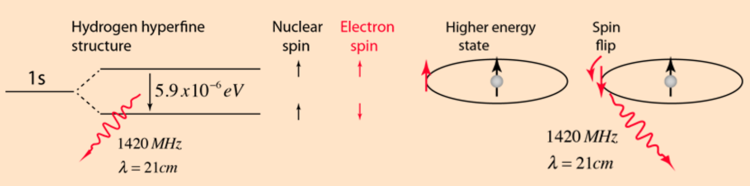

Credit: hyperphysics

- hydrogen 1s ground state slightly split due to interaction between the electron spin and the nuclear spin (hyperfine structure)
- electron transition → 1.42 GHz (21 cm) radiation ("spin flip")

Hα image of the Sun

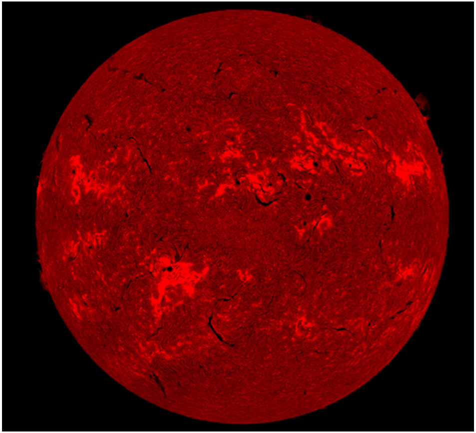

- solar full-disk image centered on the Hα line at a wavelength of 6562.8 $\AA$ in air (optical filter for light)

“False-color” images

- for an image at one particular wavelength (e.g., a specific radio emission line such as H 21-cm), we can assign a different color depending on the intensity of the signal

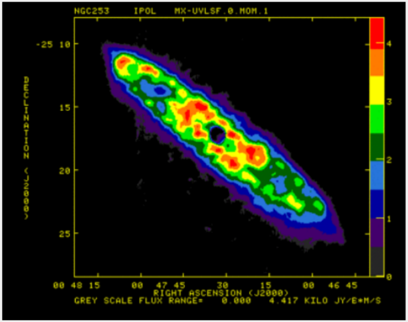

Credit: Koribalski, Whiteoak “& Houghton (1995)

red = higher localization of H1 and purple = little detection of H1

- for a continuum image, we can assign a different color to each frequency (or wavelength)

Centaurus A (Cen A)

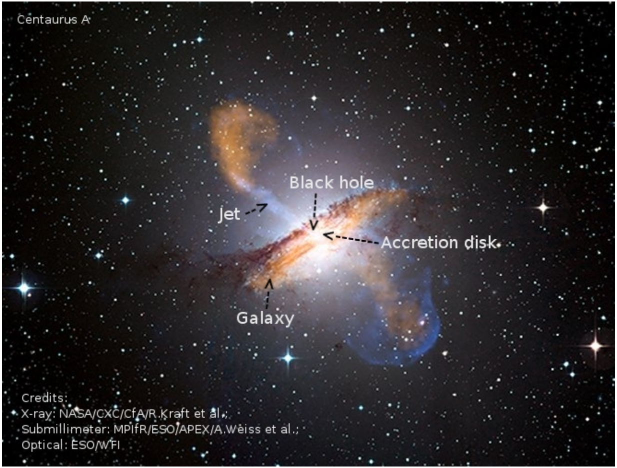

Credits:
X-ray: NASA/CXC/CfA/R.Kraft et al.;
Submillimeter: MPIfR/ESO/APEX/A.Weiss et al.;
Optical: ESO/WFI

- Cen A = the closest active galactic nucleus (AGN)
  $d \sim 3.5$ Mpc (1 pc $\sim 3 \times 10^{18}$ cm), $M_{\rm BH} \sim 5.5 \times 10^7 \; M_\odot$
- composite image (X-ray, optical, and radio)

Centaurus A (Cen A)

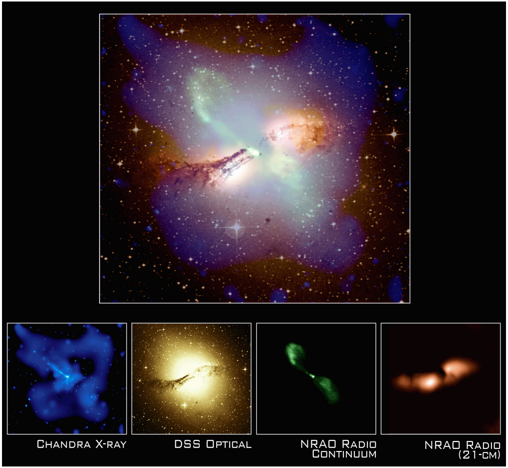

- Cen A = the closest active galactic nucleus (AGN) $d \sim 3.5$ Mpc (1 pc $\sim 3 \times 10^{18}$ cm), $M_{\rm BH} \sim 5.5 \times 10^{7}\ M_{\odot}$
- composite image (X-ray, optical, and radio)

EHT image of the jet launching region in Cen A

- jet is brighter at the edges compared to the center: edge-brightening
- phenomenon is known from other jets, but it has never been seen so pronouncedly before
- this jet-edge brightening does not solve the jet-creation mystery, but does imply that the particle outflow is confined by a strong pressure – possibly involving a magnetic field

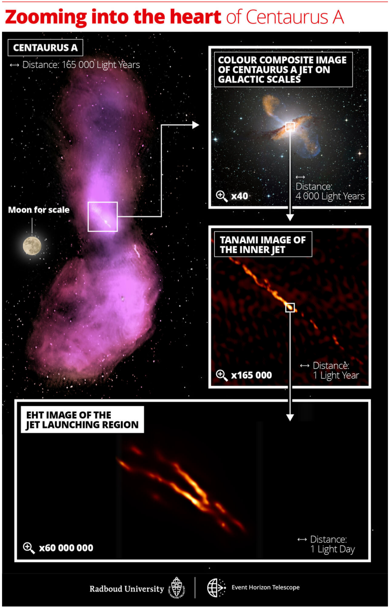

Relativistic jets in AGN

- supermassive spinning black hole ($M \sim 10^7 - 10^9\, M_\odot$)
- surrounded by an accretion disk
- relativistic plasma jets: $v_{\rm jets} \sim 0.9 - 0.995\, c$
- Lorentz factor: $\Gamma \sim 2 - 10$
- $\Gamma = \beta\gamma_0$, with $\beta = v/c$ and $\gamma_0 = (1-\beta^2)^{-1/2}$

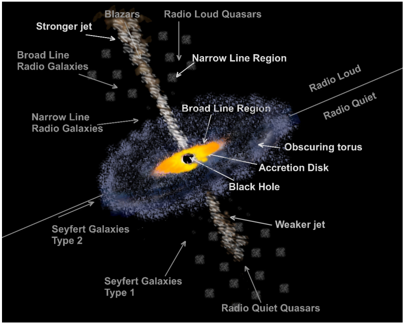

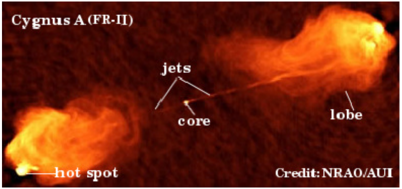

Credit: NRAO/AUI

Relativistic jets in AGN

- broad lines with widths up to 10^4 km s^{-1}
- narrow lines with a width $\sim$ 100 km s^{-1}
- jets can inflate lobs of plasma
- from interaction of lob plasma with IGM → shocks → hot spots excess emission by accelerated particles

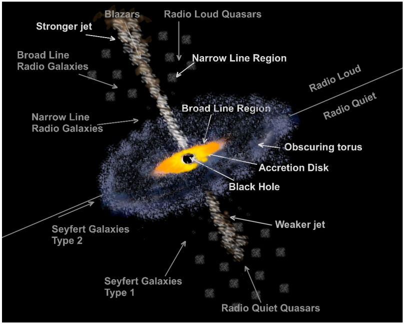

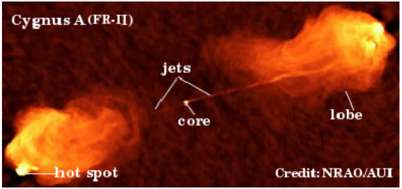

Credit: NRAO/AUI

AGN spectra in optical domain

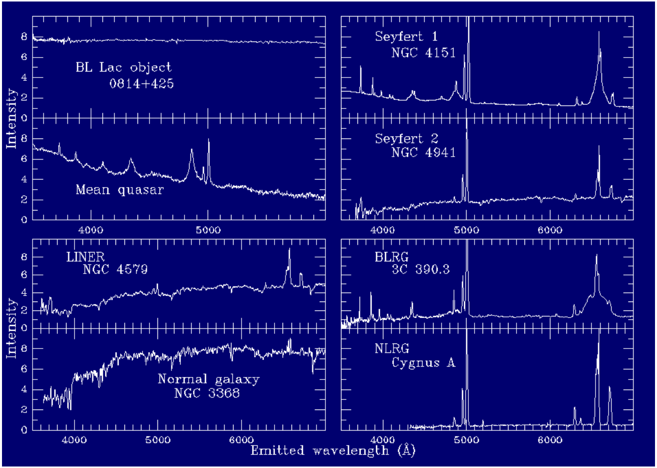

Relativistic jet in M 87

$D \sim 16$ Mpc, $M \sim 6.5 \times 10^7 M_\odot$

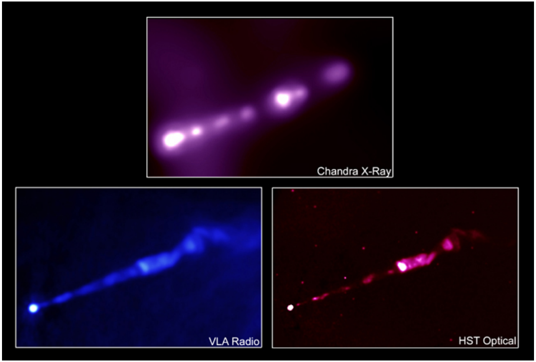

- synchrotron radiation in electromagnetic domain (images: from X-ray to radio)

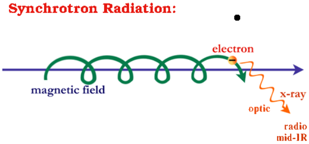

Relativistic jet in M 87

- first image of a BH
- high resolution: seeing an apple on the Moon
- this event horizon-scale image shows a ring of glowing plasma with a dark patch at the center → shadow of BH
- enhanced brightness on the southern side of the ring can result from the Doppler beaming of mildly relativistic plasma flow that is approaching the observer

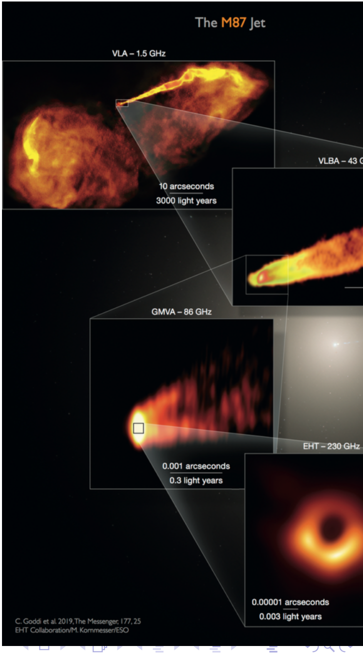

C. Goddi et al. 2019, The Messenger, 177, 25
EHT Collaboration/M. Kornmesser/ESO

Blandford-Znajek mechanism (1977)

- Electromagnetically extraction of energy and angular momentum of a BH ("BH dynamo" mechanism) → the energy flux of the jets is provided by conversion of the BH rotational energy into Poynting flux, which is then dissipated at large distances from the BH by current instabilities

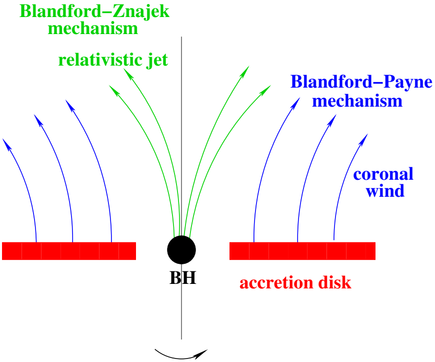

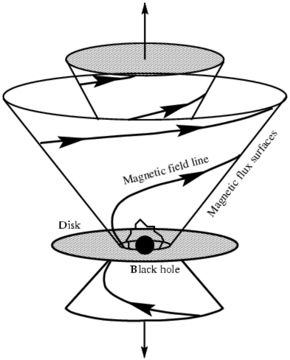

Blandford-Payne mechanism (1982)

- MHD flow – the jet can be launched and collimated by centrifugal and magnetic forces – the disk particles are driven upwards by the gradient of the pressure in the disk to fill the corona around the disk and are further accelerated by the gradient of the magnetic pressure

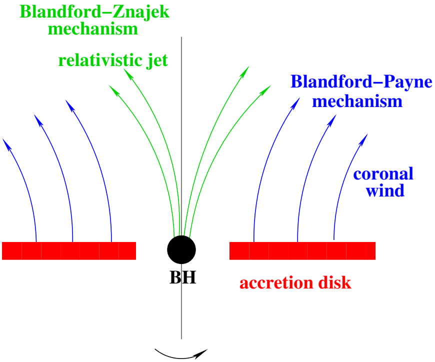

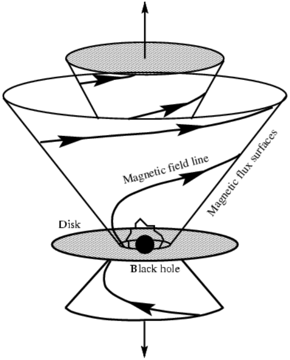

Gamma-ray burst jets

- GRBs are the most extreme explosions in Universe
- they release $\sim 10^{55}$ erg within a few secs as γ-rays
- long (> 2 seconds) GRBs and short (< 2 seconds) GRBs
- long GRBs: deaths of massive stars
- short GRBs: merger of two compact objects (neutron stars or black holes)
- furthest GRB at redshift z=9.4 ($\sim$ 13.14 billion years ago)

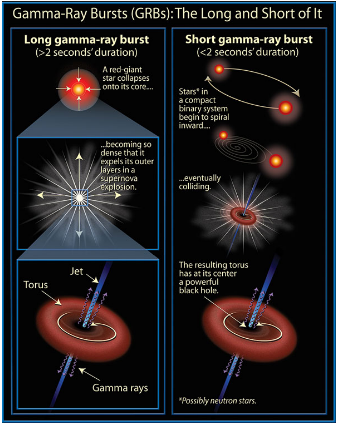

Figure: www.nasa.gov

Gamma-ray burst (GRB) jets

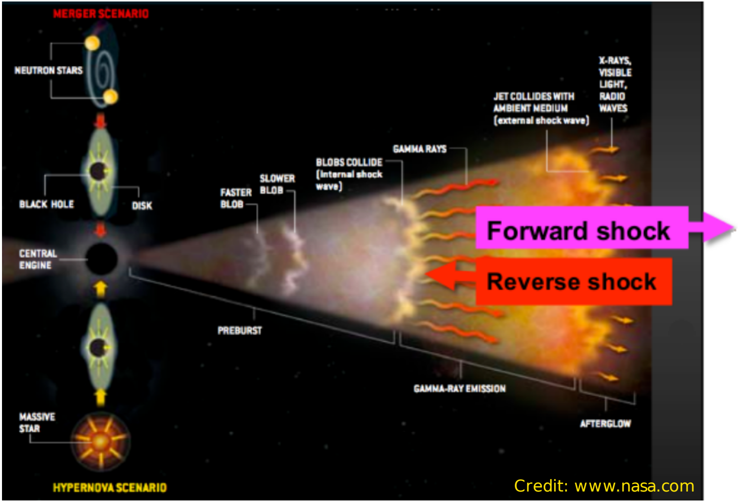

Figure: Image credit: www.nasa.gov

Spectra of gamma-ray bursts

- Present: Fermi (GLAST Burst Monitor, GBM, & Large Array Telescope, LAT) & Swift (Gamma-ray burst monitor, X-ray, UV/optical instruments)

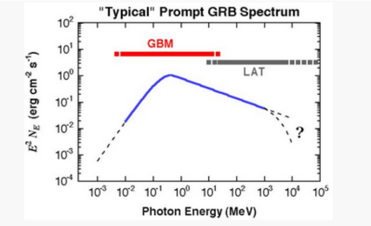

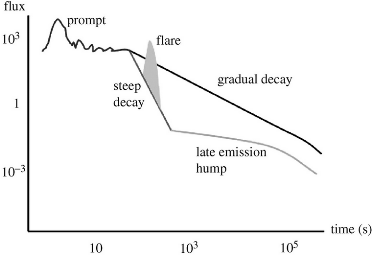

- prompt spiky emission, primary observed in the keV-MeV with no preferred pattern in the lightcurves
- emission is fallowed by a smooth afterglow, observed in X-ray, optical, radio with non-thermal spectra

Astrophysical jet plasma in the kinetic limit

- collisionless plasma: diffuse, high temperature plasma
  - large free path of particles, larger than, e.g., the gyroradius
- instabilities arise from the interaction between particles and the waves that they produce, and not from collisions between particles
- examples of kinetic (or micro)instabilities driven by anisotropy of the particle velocity distribution function (**Weibel, Kelvin-Helmholtz, & Mushroom**):
  - electromagnetic instabilities: Weibel instability
    - develops inside the jet
    - shows current filaments
  - velocity shear layer instabilities: Kelvin-Helmholtz & Mushroom instabilities
    - develop at the jet interface with the ambient medium
    - show vortex- and "mushroom"-like structures

Astrophysical jet plasma in the kinetic limit

- collisionless plasma: diffuse, high temperature plasma
  - large free path of particles, larger than, e.g., the gyroradius
- instabilities arise from the interaction between particles and the waves that they produce, and not from collisions between particles
- examples of kinetic (or micro)instabilities driven by anisotropy of the particle velocity distribution function (**Weibel, Kelvin-Helmholtz, & Mushroom**):
  - electromagnetic instabilities: Weibel instability
    - develops inside the jet
    - shows current filaments
  - velocity shear layer instabilities: Kelvin-Helmholtz & Mushroom instabilities
    - develop at the jet interface with the ambient medium
    - show vortex- and "mushroom"-like structures

Astrophysical jet plasma in the kinetic limit

- collisionless plasma: diffuse, high temperature plasma
  - large free path of particles, larger than, e.g., the gyroradius
- instabilities arise from the interaction between particles and the waves that they produce, and not from collisions between particles
- examples of kinetic (or micro)instabilities driven by anisotropy of the particle velocity distribution function (**Weibel, Kelvin-Helmholtz, & Mushroom**):
  - electromagnetic instabilities: Weibel instability
    - develops inside the jet
    - shows current filaments
  - velocity shear layer instabilities: Kelvin-Helmholtz & Mushroom instabilities
    - develop at the jet interface with the ambient medium
    - show vortex- and "mushroom"-like structures

Astrophysical jet plasma in the kinetic limit

- collisionless plasma: diffuse, high temperature plasma
  - large free path of particles, larger than, e.g., the gyroradius
- instabilities arise from the interaction between particles and the waves that they produce, and not from collisions between particles
- examples of kinetic (or micro)instabilities driven by anisotropy of the particle velocity distribution function (**Weibel, Kelvin-Helmholtz, & Mushroom**):
  - electromagnetic instabilities: Weibel instability
    - develops inside the jet
    - shows current filaments
  - velocity shear layer instabilities: Kelvin-Helmholtz & Mushroom instabilities
    - develop at the jet interface with the ambient medium
    - show vortex- and "mushroom"-like structures

Astrophysical jet plasma in the kinetic limit

- collisionless plasma: diffuse, high temperature plasma
    - large free path of particles, larger than, e.g., the gyroradius
- instabilities arise from the interaction between particles and the waves that they produce, and not from collisions between particles
- examples of kinetic (or micro)instabilities driven by anisotropy of the particle velocity distribution function (**Weibel, Kelvin-Helmholtz, & Mushroom**):
    - electromagnetic instabilities: Weibel instability
        - develops inside the jet
        - shows current filaments
    - velocity shear layer instabilities: Kelvin-Helmholtz & Mushroom instabilities
        - develop at the jet interface with the ambient medium
        - show vortex- and "mushroom"-like structures

Weibel instability

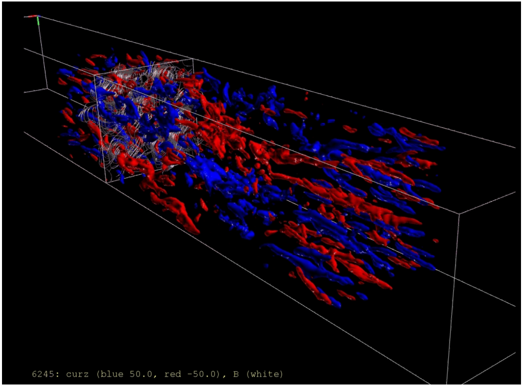

- Weibel instability can generate magnetic fields from scratch and produce collisionless shocks, where particles are accelerated and radiation is emitted (Nishikawa 2012)

Kelvin-Helmholtz and Mushroom instabilities (KHI, MI)

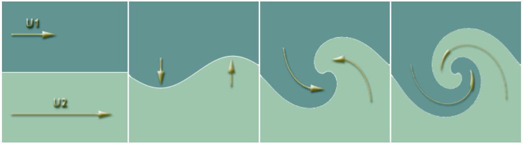

Development of KHI at velocity shears

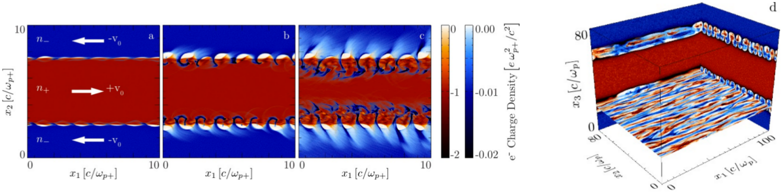

PIC simulation of counter-stream flows (Alves 2012)

Left: KHI & Right: MI

Calculating radiation spectra directly from PIC simulations

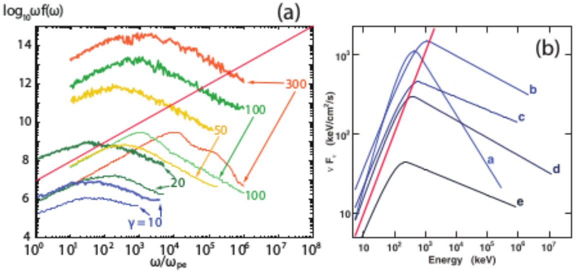

- (a) synthetic PIC spectra for Lorentz factor 10, 20, 50, 100, and 300 with cold (thin lines) and warm (thick lines) electron jets (Nishikawa et al. 2009)
- (b) modeled Fermi spectra at early (a) to late (e) times of GRB 080916C (Abdo et al. 2009)

Simulation setup (Nishikawa+ 2020, Meli, Nishikawa+ 2022)

- inject a relativistic ($\gamma_{\mathrm{jt}} = 15$) plasma jet into an ambient plasma at rest
- both of them are electron-proton plasmas
- larger simulation size than before with grid size large enough to allow for growing kinetic instabilities:

  $(L_x, L_y, L_z) = (1285\Delta, 789\Delta, 789\Delta)$, where Δ is cell size

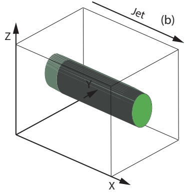

- initial toroidal magnetic field (eqs. from Mizuno et al. 2015)
- jet head with a flat-density top-hat shape

Calculation of the synthetic spectra

- for particle acceleration: 2D plots of the Lorentz factor of jet electrons (Meli, Nishikawa+ 2022)
- $e^{\pm}$ jet with $r_{\rm jt} = 100\Delta$ at $t = 900\,\omega_{\rm pe}^{-1}$

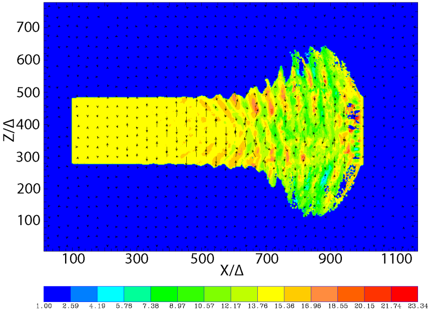

Calculation of the synthetic spectra

- patterns of the Lorentz factor coincided with the changing directions of local, generated magnetic fields
- arrows (black spots) show magnetic fields in (x, z) plane

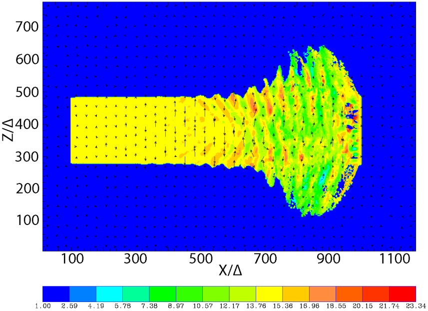

Calculation of the synthetic spectra

- MI is excited combined with a kKHI, while the produced quasi-steady E x modulates the jet particles

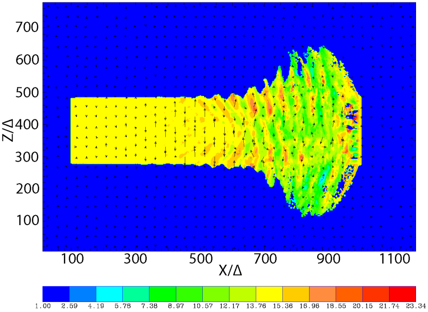

- wider jet $r_{\mathrm{jt}} = 100\Delta$
- method based on calculated the retarded potentials

  (Nishikawa et al. 2009, Hededal 2005)

$$\frac{d^2W}{d\Omega d\omega} = \frac{\mu_0 c q^2}{16\pi^3}\left| \int_{-\infty}^{\infty} \frac{\mathbf{n}\times[(\mathbf{n}-\beta)\times\dot{\beta}]}{(1-\beta\cdot\mathbf{n})^2} e^{\frac{i\omega(t' - \mathbf{n}\cdot\mathbf{r}_0(t')}{c}} dt' \right|^2$$

- select about 5000 jet electrons and follow them for 5000 steps ($\Delta t = 0.005\ \omega_{\mathrm{pe}}^{-1}$)

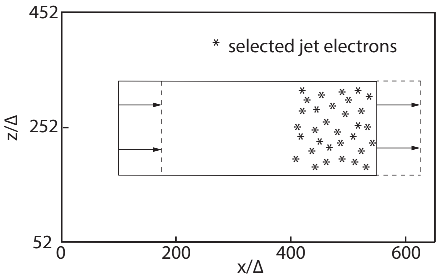

- for $e^{\pm}$ plasma jets with low ($\gamma = 15$) Lorentz factor and weak ($b_0 = 0.1c$) initial toroidal magnetic field
- (a) for head-on radiation (red for jet, blue for ambient) and 5°-off axis radiation (orange for jet, light blue ambient)
- (b) for head-on radiation (red lines) and 5°-off axis radiation (orange lines) for smaller simulations
- dashed line corresponds to the Nyquist frequency (beyond which we have distortions)

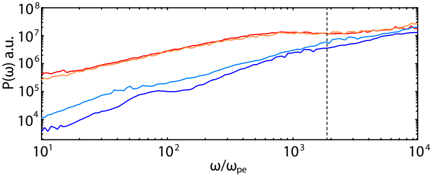

(*a*)

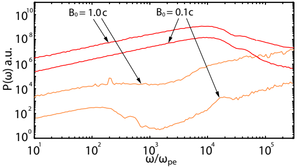

(*a*)

- phase-space distribution of jet and ambient electrons
- randomly pick-up electrons at the jet head for calculating radiation, there we have less accelerated particles in our sample
- start to develop a routine to collect the fastest particles

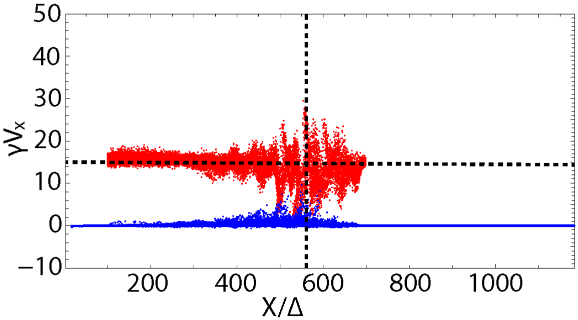

GRPIC jet formation - Hirotani, Nishikawa 2022

- initial setup: pairs in a Kerr metric for a rotating BH with uniform magnetic field (Wald solution)
- magnetic field lines (white curves) and the pair density (color) on the poloidal plane near the horizon

Magnetohydrodynamics (MHD)

- couples Maxwell's equations of electromagnetism with hydrodynamics to describe the macroscopic behavior of conducting fluids such as plasmas
- assumes that the particle gyroradius is small
- assumes the plasma is fully ionized (limited applicability to weakly ionized plasmas like the photosphere and chromosphere of the Sun)
- assumes that collisions are frequent enough so that the particle distribution function is Maxwellian (not always true, e.g., in solar wind)
- assumes no resistivity, viscosity, thermal conduction, or radiative cooling for the ideal MHD
- radiation cannot be calculated directly from the simulations - need to add a ray-tracing code

MHD equations

- MHD equations describe the motion of a conducting fluid interacting with a magnetic field
- closed system of PDE that couples magnetic field **B** with fluid velocity **v**, mass density ρ and thermal pressure p
  - continuity equation for mass conservation
  - momentum conservation
  - energy conservation
  - induction law gives the variation of magnetic field in time

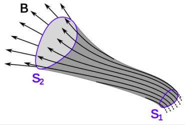

  - impose the non-existence of magnetic monopoles
  - include ecuation of state for fluid (to close the system of equations)
- to solve the system need to impose initial and boundary conditions
- include gravity for jet formation

Formation of jets from black holes with GRMHD

(Click to play movie)

- General Relativistic Magnetohydrodynamic simulation of jet formation from black holes (Duțan, Mizuno, & Nishikawa, PhD 2011)

GRMHD jet formation - Gammie's group (2003+) HARM code

- Monika Moscibrodzka (2013+): HARM code + GR ray-tracing
- Modeling emission of M87 jet: 43GHz images of a fiducial model ($a = 0.94$, $P_\mathrm{j} = 3 \times 10^{43}$ erg s^{-1}) observed at various inclination angles

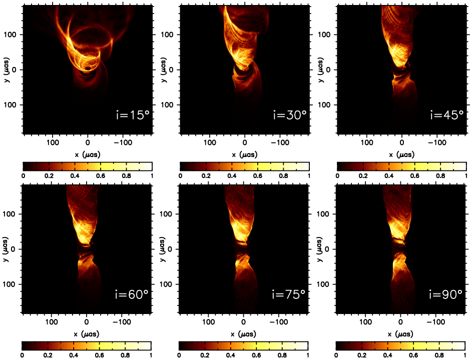

GRMHD jet formation - Gammie's group (2003+) HARM code

- Monika Moscibrodzka (2013+): HARM code + GR ray-tracing
- Modeling emission of M87 jet: 43GHz images of a fiducial model ($a = 0.94$, $P_{\rm j} = 3 \times 10^{43}$ erg s^{-1}) observed at various inclination angles

Conclusions

- PIC (microscopic, kinetic level) & MHD (macroscopic level) both can be used to describe relativistic jets
- PIC is limited to low density, energetic plasmas to resolve Debye length and requires many particles per cell
- PIC can explain the generation of magnetic field, particle acceleration, and emission of radiation in a self-consistent way, MHD does not
- Techniques to bridge the divide between MHD and PIC have been slow to develop
- Hybrid codes (MHD+PIC) has been develoved (MHD for treating protons as a fluid and PIC for electrons)
- MHD is computationally fast but approximate, PIC is (more) accurate but slow